RSC Advances

RSC Publishing

PAPER

Non-specific clustering of histidine tagged green fluorescent protein mediated by surface interactions: the collective effect in the protein-adsorption behaviour†

Cite this: *RSC Advances*, 2013, **3**, 10479

Tomasz D. Sobieściak* and Piotr Zielenkiewicz

The chemically programmed non-fouling surfaces were used to observe the surface assembly behaviour of hexahistidine tagged Green Fluorescent Protein (His-GFP) as a model protein. In this particular case, site-selective physisorption of His-GFP was achieved in the absence of metal ions. This preference does not arise from surface charge, wettability or topographic differences between regions. We found that His-GFP has a tendency to centre into an array of marked squares and acquires a template shape on the entire non-fouling surface when both the internal and surrounding areas present carboxylate groups. This surface-directed organization of protein in assemblies is an unusual example of non-specific molecular interactions transfer to a higher scale objects organization. Furthermore, we performed a proof-of-concept study for the autonomous formation of protein microarrays with uniform orientation of the tagged protein molecules on the surface. Periodic protein microarrays were formed spontaneously within about one minute after the deposition of a few drops of protein solutions on the substrate. We propose a simple, gentle and cost-effective approach to fabrication of protein microarrays, which can be done by the end-user. This phenomenon of collective protein clustering into large scale patterns may help to assess experimentally how the peripheral proteins arrange into separate domains of the cell membrane.

Received 1st May 2013,
Accepted 9th May 2013

DOI: 10.1039/c3ra42154f

www.rsc.org/advances

Introduction

In living systems, most proteins exert their functions as members of protein complexes. Assembly is included in many biological processes and is tightly regulated by adaptor proteins or switch molecules.[1] Currently, a cell-free on-chip synthesis and assembly of proteins are emerging areas of research.[2,3] Controlled adsorption of protein on surface is crucial in a plethora of applications from biosensors to tissue engineering. Micropatterned surfaces are used to modulate the cell-extracellular matrix (ECM), cell-cell and cell-ligand interactions and as biocompatible platform in tissue engineering.[4] Self-assembled monolayer (SAM) surfaces were successfully applied as a simplified model system to mimic the communication between the cell surface and the protein.[5] Protein micropatterns were proposed for assessment of intercellular protein-protein interactions.[6]

The understanding of how proteins assemble into functional cell machinery is currently of major interest in synthetic biology.[7] Little is known about the process of cluster formation of proteins in a cell membrane. Changes in the co-localization and local accumulation of membrane peripheral proteins modulate the intercellular signalling. It is unclear why the proteins have tendency to aggregate in association with membranes instead of to diffuse randomly.

Protein islands model of a plasma membrane structure assumes that the receptor proteins are clustered into aggregates in the cell membrane.[8] These protein clusters are involved in intercellular signal transduction. For example, co-localization of signalling molecules in the microclusters in the plasma membrane upon antigen recognition is essential for the activation of early immune response.[9] Clustering of the plasma membrane proteins was defined as a process which leads to a non-random distribution of unstable protein complexes without binding between the components and differs from the direct oligomerization process that forms stable complexes.[10] However, it is still unclear how the protein membrane clusters are formed. There is a need for experimental simplified model systems useful for the assessment of the formation of membrane proteins micropatterns and clusters which allow elucidating the physical principles underlying the clustering process.[11]

Physisorption of protein on a solid support is usually nonspecific and involves dynamic conformational change and

Institute of Biochemistry and Biophysics, Polish Academy of Sciences, Pawińskiego 5a, 02-106 Warsaw, Poland. E-mail: tomasz_s@ibb.waw.pl

† Electronic supplementary information (ESI) available: additional fluorescence microphotographs. See DOI: 10.1039/c3ra42154f

reorientation. Many simulation models and theories describe protein adsorption process and determine the driving force for protein motion on the surface.[12] The main question is: how to change the behaviour of adsorbing individual proteins and attain a collective effect as spontaneous arrangement of proteins in selected regions of surface. Integration of proteins in ordered clusters on a surface can be guided by external stimuli (*e.g.* electric field, light) or can be directed by using surface templates. The latter is facilitated by the low energy barrier to mobility of objects on a smooth surface. Surface-directed protein adsorption is regulated through modulation of the protein-water-surface interaction. Protein clusters or networks are most often achieved experimentally in an oligomerization process[13–15] through shape complementarity or with enhancement by molecular junctions. Self-assembly techniques including particle lithography[16] and DNA-assisted assembly[17] were proposed for periodic organization of proteins on a surface.

Recently, passive or active assembly has attracted much attention as a tool for organization of objects in more complex spatial systems and a two dimensional pattern on a surface. Programmed self-assembly[18] is an attractive route for constructing engineered systems in nano- and micro-scales.[19,20] A high level of control over assembly of colloidal micro- and nano-objects is required to achieve ordered clusters and dedicated patterns observable in a higher scale. Final global behaviour of a system in macroscale is established on a local microlevel of interacting objects. Assembly of these objects involves interplay of attractive and repulsive forces between the components which predominate over random interactions. In the last decade, much interest has been devoted to direction of colloidal particles selectively into desired surface regions and formation of highly ordered microstructures.[21] Surface-directed and site-selective assembly has been achieved by use of predefined templates fabricated by top-down approaches. Permanent fixation of assemblies to surface is often performed as the last step of the process. This is facilitated by specific interactions which strengthen binding of desired components to template pattern. Organization of colloidal particles on a surface is controlled by division of substrate into hydrophobic and hydrophilic regions, charge differentiation of surface and by invoking molecular recognition. The preference of colloidal polymer particles for specific regions was described as a good model for mesoscale object organization.[22] In this work, site-selective formation of colloidal assemblies was demonstrated to depend on pH and location of chemical functionalities on lattice patterned silane layers, *i.e.* carboxy-functionalized particles exhibit preference for selected areas, and after pH change the particles completely change their adsorption preference to opposite regions.

Two-dimensionally structured SAMs have been used extensively for fabrication of surfaces dedicated for spatial positioning of proteins.[23] Basic prerequisites are that selected parties of surface should completely resist protein adsorption or have selectively reversible protein binding properties. Nonspecific adsorption to microstructured surfaces is commonly controlled by division of surface into hydrophobic and hydrophilic regions. The difference in surface energy between these regions allows for selective attachment of proteins. Surface energy of the SAMs can be modulated by change of the reactive end group of monolayer. Typically, a surface is divided into a separated region where proteins adhere and a non-fouling region that prevent protein adsorption. Although bovine serum albumin (BSA) is widely employed for the passivation of a surface, this strategy has some limitations associated with denaturation of the blocking protein and inability to present ligands in a controlled and oriented manner. The optimal result is obtained with SAMs contained poly- or oligo-ethylene glycol chains (PEG or OEG), which resist non-specific protein adsorption, mixed with chains terminated by affinity ligands, which can selectively attach tagged proteins.[24] Moreover, OEG coated surfaces prevent unfolding of proteins after adsorption.[25]

Currently, three major strategies predominate in fabrication of protein micropatterns: the first is based on direct forced transfer of protein into a desired area of surface.[26] However, this technique is good enough only for immobilization of antibodies, ferritin or strepatavidin. In the second, less destructive indirect approach proteins bind to the printed regions of SAMs with terminal polar groups[27] or *via* specific recognition.[28,29] Among affinity ligands metal chelators are successfully applied for strengthening the specific interaction and reversible immobilization of proteins on surfaces *via* oligohistidine extension.[30] The interaction with histidine-tagged proteins can be selectively switched by adding or removing the metal ion. The third of the popular approaches requires a robotic spotter.[31] Control of protein assembly on a surface in a desired region in a single-step, rapid and energy efficient process without protein damage and with minimal non-specific adsorption is one of the demands of proteomics.[32]

Here, we show that the clustering of proteins is mediated by non-specific interactions between proteins and is facilitated and guided by surface-mediated interactions. We provide evidence that protein assembly can be site-selectively and non-specifically surface-driven. The assembly process is autonomous and occurs with omitting of shape complementarity and/or intermolecular junctions between objects. His-GFP organize in ordered array on a template which does not contain any active groups responsible for selective capturing of objects as in typical directed assembly. Moreover, regioselectivity of protein binding to surface regions does not arise from surface chemistry (charge), wettability or topographic differences between regions. The template was fabricated by liquid deposition of two types of trialkoxysilanes with chemical differentiation of regions by microcontact printing (μCP) technique.[33] The chip was designed as an array of 2500 squares. The micropatterned substrates have the entire surface coated with the same OEG-silanes mixed with silanes presenting specific functional groups. We show that protein after initial covering of the entire non-fouling surface spontaneously collocates in an ordered micropattern of squares,

earlier programmed by μCP, during a one-minute process. Direction of protein transfer can be programmed by functionalization of surface with common chemical groups. We found that protein adsorption can be regulated non-specifically.

In this work, adsorption of Green Fluorescent Protein (GFP) as a model protein[34] on the surface in designed pattern is demonstrated by using fluorescence microscopy. GFP is also a good indicator for the biocompatibility of materials since its unfolding is correlated with lack of fluorescence. Moreover, the usefulness of GFP microarray in the detection of protein-protein interactions is well documented.[35] Because the whole surface of chips is coated by mixed SAMs, there are small differences between inner and outer area of squares. Therefore, protein adlayer on the surface should be seen in Atomic Force Microscopy (AFM) imaging as an increase in height of the covering layer. X-ray photoelectron spectroscopy (XPS) was used to characterize the structured SAMs before immobilization of protein. Internal area of squares was chosen preferentially for presenting the chelating ligands: nitrilotriacetic acid (NTA) and triazacyclononane derivative (tacn-bis(formyl)). A water-soluble, non-reactive tacn-bis(formyl) ligand was prepared by the double selective approach.[36] The progress of reactions in this approach is programmed by its organization resembling a self-directed system.

Materials and methods

Materials

All solvents and reagents were obtained from commercial sources and used as received without further purification, unless otherwise stated. Ultrapure water (MilliQ water) was used throughout. Phosphate buffered saline (PBS) (50 mM/100 mM NaCl), pH 7.5 was prepared from monobasic and dibasic sodium phosphates. Recombinant His_6-tag GFP was purchased from Upstate Biotechnology. Texas Red conjugated BSA was obtained from Invitrogen. FITC-Con A was supplied by Sigma-Aldrich. PDMS stamp was purchased from Platypus Technologies.

Preparation of glass chips

Glass coverslips were cleaned in Piranha solution (**Caution:** Piranha solution is extremely corrosive and can react violently with organic compounds), washed with MilliQ water, ethanol and subsequently immersed into 3 : 1 mixture of methoxy-terminated hexaethylene glycol-trimethoxysilane and amino-propyl-trimethoxysilane in toluene (10 mM) for 40 min and immersed in 5% succinic anhydride solution in DMF for 1 h. Then SAMs was functionalized by N-hydroxysuccinimide (NHS) (aqueous solution of 75 mM EDC and 15 mM NHS for 30 min) and subsequently stamped with 2-amine-2-hydroxymethyl-1,3-propanediol and backfilled with appropriate chelator (5 mg ml^{-1}). The ligand-functionalized sample was activated by immersion in Ni_2SO_4 solution (50 mM).

Protein adsorption experiments

For protein adsorption experiments, the samples prepared as described above, were incubated in His-GFP (10 μg ml^{-1}) in PBS buffer, pH 7.5 for 1 min without mixing or overnight at room temperature.

Fluorescence microscopy

The behaviour of the fluorescent proteins on the patterned glass chips was observed by fluorescence microscopy. Images were acquired with fluorescence microscope (Axio, Zeiss) and image acquisition software. Glass slide coated with mixed SAMs-the chip was incubated overnight with the appropriate protein: His-tag GFP or fluorescently labeled protein: FITC-Con A and Texas Red BSA at ambient temperature without mixing.

Atomic force microscopy

Glass slide coated with mixed SAMs was prepared as above for fluorescence microscopy observation. The chip was scanned after overnight incubation with His-GFP solution at ambient temperature. It was then immersed in PBS buffer and rinsed with distilled water. AFM experiments were performed with Agilent 5500 microscope in a commercial liquid cell. Imaging was performed in TopMac mode with Mac type II cantilevers (Agilent) at resonance frequencies near to 40 kHz in PBS buffer and at drive amplitudes of 1.5 to 2 mV. The AFM images of the area 100 μm × 100 μm were taken at a scan rate of 1 or 0.5 lines per second, and the data collection resolution was between 512 × 512 and 1024 × 1024 pixels.

X-ray photoelectron spectroscopy

XPS analysis was carried out using Scanning ESCA Microprobe (PHI 5000 VersaProbe). The surface was irradiated using an Al monochromatic X-ray source (1.3 W, 45°, 117.40 eV).

Results

In order to observe the collective effect in the protein-adsorption behaviour we need an experimental system that will allow to test the specific and non-specific interactions between proteins on the same biocompatible platform without substantial change in the structure of monolayer films. On the other hand, this system should allow for altering the chemical nature of terminal groups on selected areas of the surface. Chelating agents can acquire the characteristics of the protein capturing ligand by simple metal ion coordination. Generally, adsorption of a protein to a surface leads to the irreversible protein unfolding and loss of biological activity. Fluorescence of GFP reflects correct folding and correlates with the biocompatibility of the material.

The first experimental approach was based on specific interactions between chelating ligands and tagged protein. Micropatterned surface consisting of 100 μm × 100 μm squares separated by area of 100 μm length was fabricated by μCP. Chips had the entire area coated by OEG silane. Internal area of squares presented NTA ligand while surrounded area presented hydroxyl groups. The chip was activated by Ni^{2+} to

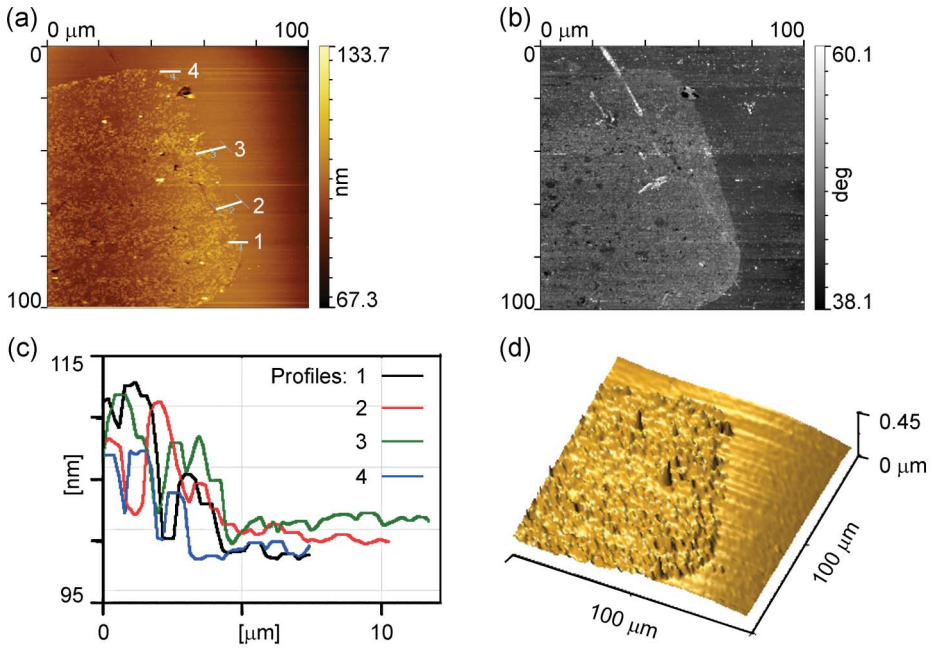

Fig. 1 AFM images of individual 1000 μm^2 area after deposition of His-GFP and its corresponding cross sectional surface profile. AFM images were collected in liquid cell in TopMac mode. Non-contact mode was chosen in order to prevent mechanical deformation and/or disruption of protein adlayer. (a) Surface with adsorbed His-GFP in the topographic mode. (b) Surface with adsorbed His-GFP imaged in the phase-contrast mode. The phase image reveals the compositional difference between the two regions. (c) Height profiles taken along the four lines marked on the corresponding AFM image (a). The difference in height between protein-coated and uncoated regions is clear. (d) AFM 3D topography image of scanned area with adsorbed His-GFP.

form the Ni-NTA complex, which are able to capture tagged GFP. In Fig. 1 we demonstrate the results obtained by the non-contact mode AFM in aqueous solution after deposition of His-GFP. In AFM scan window the fragment of one square can be observed. The topographic and phase AFM images reveal a good contrast and show that protein layer is located only over the internal area of squares presenting ligand–metal complex and the external area is extremely smooth. Fig. 1c demonstrates cross-sections corresponding to the 4 lines depicted on the topographic AFM image. Profiles reveal a height difference of 5–20 nm between the internal area of square and surrounding area. These values are comparable with GFP dimensions of 3 by 4 nm in solution and AFM measurements.[37,38] AFM 3D imaging (Fig. 1d) clearly shows that His-GFP adsorbs preferentially on the internal regions containing the ligand terminated silane. The image confirms that there is no nonspecific binding or denatured protein in the ligand free region.

Then, we show that the surface region in AFM image with adsorbed protein molecules corresponds well to the same region that exhibits His-GFP fluorescence, and further, dark regions correspond to regions without protein. Thus, for the real time observation of protein adsorption behaviour, the chip was activated by Ni^{2+}, washed and subsequently exposed to His-GFP solution in PBS buffer, pH 7.5, under microscope objective. We observed rapid self-collocation of His-GFP in array of squares (green squares in Fig. 2a). The image confirmed that there was no non-specific binding of protein in ligand-free region (dark surrounding area in Fig. 2a). Similar results were achieved after introduction to internal area of squares NTA and tacn-bis(formyl) ligands and subsequent washing (Fig. 2b and c). Additional experiments showed that binding was specific; protein desorption was observable only after washing with imidazole buffer, and complete removal of proteins from the surface was achieved after EDTA washing (see supplementary material for fluorescence microphotographs of chips (Fig. S1 and S2, ESI†)).

In the second non-specific approach, NTA ligand was not activated by metal ions. Similarly to above experiments, the glass slide was patterned to have an OEG-coated surface with hydroxy terminated silanes surrounding chelator-functionalized pattern squares. In the case of NTA (Fig. 3a) adsorption of His-tagged protein was always observed in the surrounding area of squares functionalized by NTA. Carboxylate groups of NTA direct protein to the outer area. Fig. 3a also demonstrates the image at higher magnification of NTA-functionalized surface pattern. The border line of square area coated with protein (green area) and uncoated (dark area) is clearly visible. There is no detectable protein fluorescence in the internal area of squares. Furthermore, we show that the pattern formed by His-tag GFP is changed depending on the presented chemical functional groups on a surface. Fig. 3b shows the results of self-collocation of His-GFP on a surface prepared as above with NTA-functionalized internal area of squares (without chelated metal ions), but surrounded by carboxyl terminated silanes mixed with OEG-silanes. (Carboxylate groups were introduced by stamping with glycine). Carboxylate group introduced in the surrounding area of squares seems to direct the His-GFP from

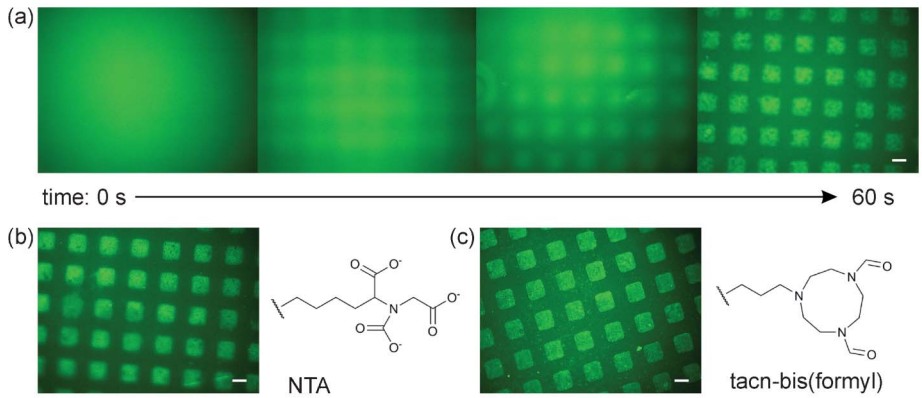

Fig. 2 Fluorescence microphotographs show a part of the surface with hexahistidine tagged GFP selectively captured into the high-contrast micropattern (magnification 100 ×). Scale bar represents 100 μm. (a) Sequence of microphotographs-from 0 s to 60 s after loading of His-GFP on the whole surface of chip functionalized with Ni-NTA ligand in the internal area of squares. Protein was deposited directly under fluorescent microscope objective and observed immediately. Images are arranged in a series of pictures taken at a specific time. (b) Micropatterned surface with His-GFP bonded to NTA chelated nickel ions after overnight incubation and a subsequent washing step. (c) As in (b), but with tacn-bis(formyl)-Ni.

external to internal area of squares. Self-collocation of His-GFP in array of squares was also observed in the case of the tacn-bis(formyl)-functionalized chip (see supplementary material for sequence of microphotographs (Fig. S3, ESI†)).

Microarrays of covalently bound proteins: FITC-Con A, Texas Red BSA and His-tag GFP (see supplementary material for fluorescence microphotographs of covalently bonded protein on chips (Fig. S4, ESI†)) were fabricated by the same method, but internal area of squares was functionalized with NHS

The ability of the prepared surface to preserve protein conformation was confirmed by denaturation of protein by low pH buffer and subsequent successful refolding of covalently bound His-GFP (Fig. 4). A control experiment was performed as in ref. 25, but no data is shown.

The surface elemental composition was probed by X-ray photoelectron spectroscopy (XPS). Fig. 5 shows the results for the NTA-functionalized mixed SAMs microcontact printed on a glass surface. SXI images show that the border line of squares is sharp and well-defined. Moreover, elemental distribution of carbon and oxygen was demonstrated using XPS imaging. Clearly, O1s signals predominate in the area corresponding to the area with introduced hydroxyl groups. Elemental analysis well reveals the character of mixed SAM and provides clear evidence of patterned surface. The XPS mapping was also performed on the same sample in order to detect and perceive the distribution of nickel ions chelated to the surface NTA groups. It was expected that nickel would be in oxidized forms,

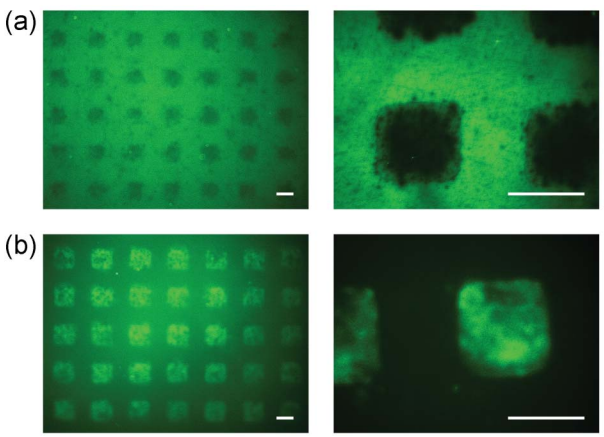

Fig. 3 Results of nonspecific collocation of His-GFP: Fluorescence micrographs showing micropatterns formed after collocation of His-GFP. Left image at magnification 100 ×. Right image at magnification 400 ×. Scale bar represents 100 μm. (a) Fluorescent images of glass slide after 1 min collocation of His-GFP. Internal area of squares presents NTA ligands without Ni ions while surrounding area presents hydroxyl groups. (b) Fluorescent images of glass slide with whole area presenting carboxylate groups mixed with OEG chains.

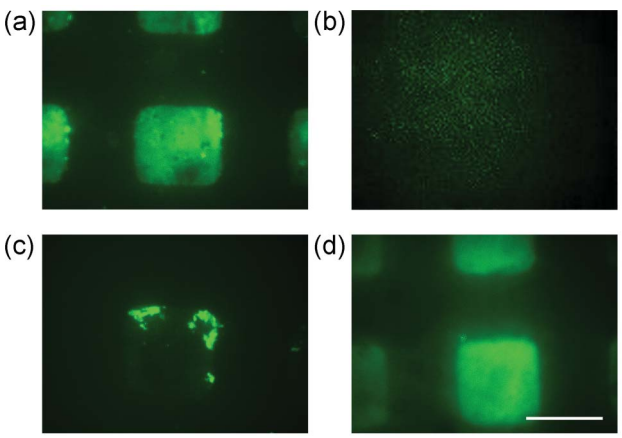

Fig. 4 His-GFP covalently bound to the micropatterned surface; incubation under denaturing condition and subsequent refolding of protein (magnification 400 ×). Scale bar represents 100 μm. (a) Surface with bound protein. (b) After incubation under denaturing conditions (25 mM acetic acid, pH 4.0) for 5 min. (c) After incubation in refolding buffer (50 mM PBS, 20% sucrose, 10% glycerol) for 30 min. (d) After incubation in refolding buffer for 3 days.

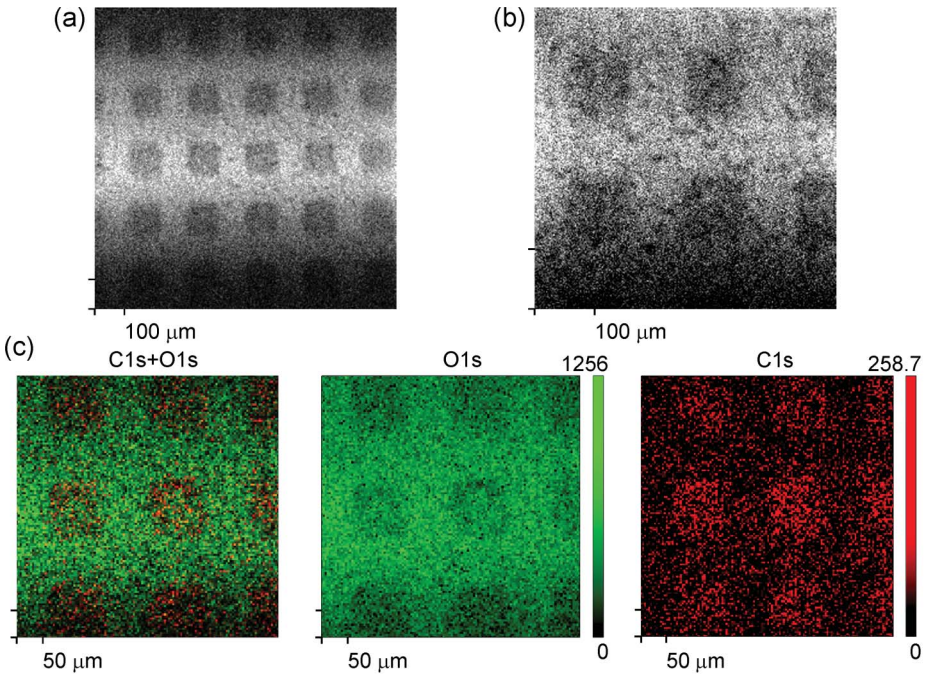

Fig. 5 XPS analysis of micropatterned surface functionalized by NTA ligand (surface without protein): X-ray Beam Induced Secondary Electron Images (SXI) of 1000 × 1000 μm (a) and 500 × 500 μm (b) areas. (c) XPS map of carbon and oxygen (left) composed of the individual C 1s (red) and O 1s (green) images (right). The maps were generated over the area of 500 × 500 μm using Scanning ESCA Microprobe.

mainly as $Ni(OH)_2$. Detection of nickel ions was unsuccessful due to the high signal to noise ratio of the XPS scans (data not presented). A low concentration of nickel ions could explain this case, as in similar case on a NTA-functionalized silica surface.[39] Therefore. the presence of nickel ions in the chips was confirmed by fluorescence probe studies using His-GFP (Fig. S1 and S2, ESI†).

Discussion

A series of mixed SAMs surfaces with small differences in surface chemistry of selected regions were obtained through soft lithography. The micropatterned substrates have the entire surface coated with the same OEG-silanes mixed with silanes presenting a specific functional group. In other words, both internal and external area of squares has a high resistivity to protein adsorption. Additionally, internal or external area of squares can be modified and then presents the desired functional groups-in our experiments typically hydroxyl or carboxylate groups. Internal area of squares was functionalized by chelating ligand NTA or tacn-bis(formyl) suitable for capturing histidine-tagged protein as affinity counterpart. In all experiments protein solution was deposited on the whole area of surface in the last step of the chip fabrication. In the first phase protein covered the whole surface and in the second phase it migrated into the chosen region. Non-specific electrostatic interactions were reduced by the composition of incubation buffer (sodium chloride) and by repulsions between protein and OEG chains, one of components of mixed SAMs. The immobilization of proteins on substrates was observed by fluorescence microscopy, and was confirmed by AFM imaging.

In our experiment proteins spontaneously assemble and adopt a programmed arrangement on a surface, typically in a one minute process. The structured SAMs lattice was designed to observe site-selective adsorption of proteins. His-GFP interactions with surface were probed in two attempts: specifically *via* affinity ligand and non-specifically. On surfaces functionalized with chelating ligand, assembly and disassembly can be regulated by adding small molecules (*e.g.* imidazole). Fluorescence microscopy observations have shown the preferential adsorption of His-GFP in the surrounding area of squares functionalized with NTA (without metal ion). Moreover, the His-GFP assembly was redirected into another region of surface after a small change in functionalities of presented chemical group. We show that change in protein location occurs when both internal and surrounding area of squares presents carboxylate groups. Therefore, we suppose that electrostatic interactions between negatively charged surface of GFP at pH 7.5 and interactions with positively charged imidazole groups of His-tag do not predominate. His-tag has little effect on the crystal structures of soluble proteins,[40] but experimental observations indicate that the incorporation of a His-tag may alter the solubility of the protein or its binding interactions. Protein organization into pattern on these initially programmed surfaces can be considered to be the result of minimization of interfacial free energy between micropatterned monolayer and water. For

example, some observations suggest that cell's shape is determined by energy minimization, *i.e.* cells deposited onto an array of ECM proteins spontaneously acquire shapes determined by the lattice pattern according to the landscape of local adhesion energy minima.[41] Furthermore, a physical lattice model predicts that the formation of periodic clusters in the plasma membrane is driven spontaneously.[42] Protein behaviour on a surface can also arise from interactions with the electric field generated by the surface. The driving force for protein motion in the presence of surface can be determined by attractive van der Waals interaction. Surface energy and solvent-surface interactions also induce protein transfer.[43]

Our observations indicate that complementarity of shape or structural recognition elements are not necessary for induction of protein assembly on surface and point to a passive assembly mechanism where objects lead to association due to assuming their new local thermodynamic equilibrium state. This phenomenon of collective protein clustering into large scale patterns may help to assess experimentally how the peripheral proteins arrange into separate domains of the cell membrane. For comparison, active assembly is directed by structurally imprinted program in surface chemistry and the operator can choose the predominant preferred interactions. In the plethora of protein patterning approaches, proteins are selectively captured by affinity ligands or antibodies in the desired surface region whereas the remaining surface prevents protein binding.

Conclusions

Firstly, we demonstrate a non-specific placement of the protein in a defined pattern depending on the chemical groups presented on the surface. Secondly, we present the phenomenon of directional migration of proteins to predefined areas on the whole protein repellent surface. The self-collocation of fluorescent protein after deposition on a template substrate was observed typically in a one minute spontaneous process. The combined evidence indicates that clustering of proteins is a surface-mediated process. Furthermore, this oriented gentle attachment of biomolecules onto mixed SAMs at glass surfaces is an attractive route for the development of protein arrays suitable for further direct on-plate analysis[44] by laser desorption/ionization mass spectrometry. The programmed surfaces can help elucidate how proteins are driven from solution to a surface.

Acknowledgements

T.D.S. wishes to thank Dr J. Grzyb from the Institute of Physics PAS, Warsaw, for AFM measurements and Dr W. Lisowski from the Institute of Physical Chemistry PAS, Warsaw, for XPS mapping analysis.

Notes and references

1 M. Kinoshita, C. M. Field, M. L. Coughlin, A. F. Straight and T. J. Mitchison, *Dev. Cell*, 2002, **3**, 791–802.
2 Y. Heyman, A. Buxboim, S. G. Wolf, S. S. Daube and R. H. Bar-Ziv, *Nat. Nanotechnol.*, 2012, **7**, 374–378.
3 A. W. Feinberg and K. K. Parker, *Nano Lett.*, 2010, **10**, 2184–2191.
4 B. G. Chung, L. Kang and A. Khademhosseini, *Expert Opin. Drug Discovery*, 2007, **2**, 1–16.
5 N. Horan, L. Yan, H. Isobe, G. M. Whitesides and D. Kahne, *Proc. Natl. Acad. Sci. U. S. A.*, 1999, **96**, 11782–11786.
6 M. Schwarzenbacher, M. Kaltenbrunner, M. Brameshuber, C. Hesch, W. Paster, J. Weghuber, B. Heise, A. Sonnleitner, H. Stockinger and G. J. Schutz, *Nat. Methods*, 2008, **5**, 1053–1060.
7 P. E. M. Purnick and R. Weiss, *Nat. Rev. Mol. Cell Biol.*, 2009, **10**, 410–422.
8 B. F. Lillemeier, J. R. Pfeiffer, Z. Surviladze, B. S. Wilson and M. M. Davis, *Proc. Natl. Acad. Sci. U. S. A.*, 2006, **103**, 18992–18997.
9 E. Molnár, S. Deswal and W. W. A. Schamel, *FEBS Lett.*, 2010, **584**, 4832–4837.
10 K. Radhakrishnan, A. Halasz, M. M. McCabe, J. S. Edwards and B. S. Wilson, *Ann. Biomed. Eng.*, 2012, **40**, 2307–2318.
11 S. Li, X. Zhang and W. Wang, *Biophys. J.*, 2010, **98**, 2554–2563.
12 M. Rabe, D. Verdes and S. Seeger, *Adv. Colloid Interface Sci.*, 2011, **162**, 87–106.
13 P. Ringler and G. E. Schulz, *Science*, 2003, **302**, 106–109.
14 N. D. Bogdan, M. Matache, G.-D. Roiban, C. Dobrota, V. M. Meier and D. P. Funeriu, *Biomacromolecules*, 2011, **12**, 3400–3405.
15 N. Ilk, E. M. Egelseer and U. B. Sleytr, *Curr. Opin. Biotechnol.*, 2011, **22**, 824–831.
16 J. N. Ngunjiri, S. L. Daniels, J.-R. Li, W. K. Serem and J. C. Garno, *Nanomedicine*, 2008, **3**, 529–541.
17 H. Yan, S. H. Park, G. Finkelstein, J. H. Reif and T. H. LaBean, *Science*, 2003, **301**, 1882–1884.
18 V. Uskokovic, *Adv. Colloid Interface Sci.*, 2008, **141**, 37–47.
19 M. Mastrangeli, S. Abbasi, C. Varel, C. Van Hoof, J.-P. Celis and K. F. Bohringer, *J. Micromech. Microeng.*, 2009, **19**, 083001.
20 J. I. Hahm, *J. Biomed. Nanotechnol.*, 2011, **7**, 731–742.
21 M. Grzelczak, J. Vermant, E. M. Furst and L. M. Liz-Marzan, *ACS Nano*, 2010, **4**, 3591–3605.
22 U. Jonas, A. del Campo, C. Kruger, G. Glasser and D. Boos, *Proc. Natl. Acad. Sci. U. S. A.*, 2002, **99**, 5034–5039.
23 W. Senaratne, L. Andruzzi and C. K. Ober, *Biomacromolecules*, 2005, **6**, 2427–2448.
24 D. Samanta and A. Sarkar, *Chem. Soc. Rev.*, 2011, **40**, 2567–2592.
25 B. Holtz, Y. Wang, X.-Y. Zhu and A. Guo, *Proteomics*, 2007, **7**, 1771–1774.
26 A. Bernard, E. Delamarche, H. Schmid, B. Michel, H. R. Bosshard and H. Biebuyck, *Langmuir*, 1998, **14**, 2225–2229.
27 G. P. Lopez, H. A. Biebuyck, R. Harter, A. Kumar and G. M. Whitesides, *J. Am. Chem. Soc.*, 1993, **115**, 10774–10781.
28 S. Engin, V. Trouillet, C. M. Franz, A. Welle, M. Bruns and D. Wedlich, *Langmuir*, 2010, **26**, 6097–6101.

29 G. M. Hjorto, M. Hansen, N. B. Larsen and T. N. Kledal, *Biomaterials*, 2009, **30**, 5305–5311.
30 P. Jonkheijm, D. Weinrich, H. Schroder, C. M. Niemeyer and H. Waldmann, *Angew. Chem., Int. Ed.*, 2008, **47**, 9618–9647.
31 I. Barbulovic-Nad, M. Lucente, Y. Sun, M. Zhang, A. R. Wheeler and M. Bussmann, *Crit. Rev. Biotechnol.*, 2006, **26**, 237–259.
32 P. Angenendt, J. Kreutzberger, J. Glokler and J. D. Hoheisel, *Mol. Cell. Proteomics*, 2006, **5**, 1658–1666.
33 S. A. Ruiz and C. S. Chen, *Soft Matter*, 2007, **3**, 1–11.
34 M. Zimmer, *Chem. Rev.*, 2002, **102**, 759–781.
35 T. Kukar, S. Eckenrode, Y. Gu, W. Lian, M. Megginson, J.-X. She and D. Wu, *Anal. Biochem.*, 2002, **306**, 50–54.
36 T. D. Sobieściak and P. Zielenkiewicz, *J. Org. Chem.*, 2010, **75**, 2069–2072.
37 M. Ormo, A. B. Cubitt, K. Kallio, L. A. Gross, R. Y. Tsien and S. J. Remington, *Science*, 1996, **273**, 1392–1395.
38 Z. Liu, Y. Zu, Y. Fu, Z. Zhang and R. Meng, *Microsc. Res. Tech.*, 2008, **71**, 802–809.
39 E. Kang, J.-W. Park, S. J. McClellan, J.-M. Kim, D. P. Holland, G. U. Lee, E. I. Franses, K. Park and D. H. Thompson, *Langmuir*, 2007, **23**, 6281–6288.
40 M. Carson, D. H. Johnson, H. McDonald, C. Brouillette and L. J. Delucas, *Acta Crystallogr., Sect. D: Biol. Crystallogr.*, 2007, **63**, 295–301.
41 B. Vianay, J. Käfer, E. Planus, M. Block, F. Graner and H. Guillou, *Phys. Rev. Lett.*, 2010, **105**, 128101.
42 H. Wang, N. S. Wingreen and R. Mukhopadhyay, *Phys. Rev. Lett.*, 2008, **101**, 218101.
43 P. Parhi, A. Golas, N. Barnthip, H. Noh and E. A. Vogler, *Biomaterials*, 2009, **30**, 6814–6824.
44 P. L. Urban, A. Amantonico and R. Zenobi, *Mass Spectrom. Rev.*, 2011, **30**, 435–478.

